Splice Site Contribution in Alternative Splicing of *PLP1* and *DM20*: Molecular Studies in Oligodendrocytes

Grace M. Hobson,[1] Zhong Huang,[2] Karen Sperle,[1] Erik Sistermans,[3] Peter K. Rogan,[4] James Y. Garbern,[5] Edwin Kolodny,[6] Sakkubai Naidu,[7] and Franca Cambi[8]

[1]Nemours Biomedical Research, Alfred I. duPont Hospital for Children, Nemours Children's Clinic, Wilmington, DE; [2]Department of Biochemistry and Molecular Pharmacology, Thomas Jefferson University; Philadelphia, PA, [3]Department of Human Genetics, University Medical Center, Nijmegen, The Netherlands; [4]Laboratory of Human Molecular Genetics, Children's Mercy Hospital and Clinics, Kansas City, MO; [5]Department of Neurology and Center for Molecular Medicine and Genetics, Wayne State University School of Medicine, Detroit, MI; [6]Department of Neurology, New York University Medical Center, New York, NY; [7]Neurogenetics Unit, Johns Hopkins University School of Medicine, Kennedy Krieger Institute, Baltimore, MD [8]Departments of Neurology and Neurobiology, University of Kentucky, Lexington, KY

Corresponding author:

Grace M. Hobson, PhD

Nemours Biomedical Research

Alfred I. duPont Hospital for Children

PO Box 269

Wilmington, DE 19899

Phone: (302) 651-6829

Fax: (302) 651-6899

Email: ghobson@nemours.org

ABSTRACT

Mutations in the proteolipid protein 1 (*PLP1*) gene cause the X-linked dysmyelinating diseases Pelizaeus-Merzbacher disease (PMD) and spastic paraplegia 2 (SPG2). We have examined the severity of the following mutations that were suspected of affecting levels of *PLP1* and *DM20* RNA, the alternatively spliced products of *PLP1*: c.453G>A, c.453G>T, c.453G>C, c.453+2T>C, c.453+4A>G, c.347C>A, and c.453+28_+46del (old nomenclature did not include the methionine codon: G450A, G450T, G450C, IVS3+2T>C, IVS3+4A>G, C344A, and IVS3+28-+46del). These mutations were evaluated by information theory-based analysis and compared with mRNA expression of the alternatively spliced products. The results are discussed relative to the clinical severity of disease. We conclude that the observed *PLP1* and *DM20* splicing patterns correlated well with predictions of information theory-based analysis and that the relative strength of the *PLP1* and *DM20* donor splice sites plays an important role in *PLP1* alternative splicing.

KEY WORDS

Pelizaeus-Merzbacher disease, proteolipid protein 1 gene, *PLP1*, alternative splicing, information theory, genotype-phenotype

DATABASES

PLP1 – OMIM: 300401; GenBank: AJ006976

PLP1 mRNA – GenBank: M54927

PLP1 protein – GenBank: AAA59565

PMD – OMIM: 312080

Automated Splice Site Analysis server - https://splice.cmh.edu/

INTRODUCTION

Myelin proteolipid protein 1 (PLP1) is the major intrinsic protein of central nervous system (CNS) myelin and is expressed by oligodendrocytes (Lees and Bizzozero, 1991). *PLP1* (OMIM: 300401) gene expression is activated at the time of oligodendrocyte cell differentiation and gives rise to two protein products, PLP1 and DM20, generated from the same primary transcript by joining two competing 5' splice sites in exon 3 to the same 3' acceptor site (Nave, et al., 1987). The upstream splice donor site is used in the formation of *DM20* mRNA, and a site 105 bp downstream is used in the formation of *PLP1* mRNA. The *PLP1* splice site is preferentially utilized by oligodendrocytes, whereas the *DM20* splice site is more broadly utilized by Schwann cells, the myelin producing cells of the peripheral nervous system, and some non-myelin producing cells (Campagnoni, 1988).

In addition to cell-specific regulation, *PLP1* splicing is subject to developmental regulation (Timsit, et al., 1992; Stecca, et al., 2000; Sporkel, et al., 2002). *DM20* message is expressed in the embryonic central nervous system by the oligodendrocyte progenitor cells, whereas the *PLP1* transcript is made in the postnatal period by differentiated oligodendrocytes. During myelination and adulthood, *PLP1* is the predominant message reaching a ratio of 3:1 with *DM20* (LeVine, et al., 1990; Sporkel, et al., 2002). The preferential usage of the *PLP1* splice site by differentiated oligodendrocytes suggests the existence of a specialized recognition system that favors the *PLP1* splice site selection over the *DM20* site.

Mature mRNA formation depends on the precise recognition of exon-intron boundaries through sequences at 5' splice donor site, 3' acceptor site, and branch points that allow efficient and accurate removal of introns from pre-mRNAs. The early steps of splicing involve the recognition of the splice sites by small nuclear ribonucleoprotein particles (snRNPs). The U1snRNP binds

the 5' donor site, splicing factor 1 (SF1) binds the branch points, and U2snRNP auxiliary factor binds the polypyrimidine tract and the 3' site (Smith and Valcarcel, 2000). In addition to constitutive splicing, exons can be alternatively spliced giving rise to transcript diversity and complexity generally according to a developmental or tissue-specific pattern.

Acceptor splice sites flanking alternatively spliced exons are often weak sites, and sequences contained in exons and introns favor selection of splicing by modifying the splice site recognition (Thompson, et al., 2002). Alternative splicing often results in either inclusion or exclusion of a specific exon by alternative usage of the 3' splice site. The alternative splicing of *PLP1* and *DM20* depends on the alternative usage of two 5' donor sites, one of which is intra-exonic (Humphrey, et al., 1995; Elrick, et al., 1998; Hobson, et al., 2002). Because recognition of 5' donor sites occurs processively, intra-exonic 5' splice sites similar in strength to the corresponding natural donor sites may become activated (Orkin, et al., 1983; Treisman, et al., 1983; Rogan, et al., 1998). This is consistent with the possibility that both exonic and intronic regulatory sequences might influence the preferential selection of one site versus the other.

The regulatory mechanisms that control the preferential usage of the *PLP1* splice site in oligodendrocytes are not fully characterized. We have identified a 19-bp G-rich element in intron 3 (+28/+46 downstream of the *PLP1* splice site) that controls selection of *PLP1*-specific splice site in oligodendrocytes (Hobson, et al., 2002). This element functions as an intronic enhancer of splicing and its deletion results in drastic reduction of *PLP1* splice site selection, leaving the *DM20* transcript relatively unaffected. Deletion of this element causes a disorder with both neurodevelopmental and neurodegenerative features (Hobson, et al., 2002). These findings support the importance of *PLP1/DM20* alternative splicing in normal development and maintenance of brain function. Furthermore, mutations affecting *PLP1* and *DM20* splice sites

result in clinical phenotypes typical of Pelizaeus-Merzbacher disease (PMD) and present with various degrees of severity, underscoring the importance of tight regulation of *PLP1* and *DM20* splicing.

To investigate the role of *PLP1* and *DM20* splice site strength in the regulation of *PLP1* alternative splicing, we have characterized the effect of the following mutations at conserved bases in and around the *PLP1* and *DM20* splice sites in the selection of the 5' donor sites in developing oligodendrocytes in vitro: c.453G>A, c.453G>T, c.453G>C, c.453+2T>C, c.453+4A>G, c.347C>A, and c.453+28_+46delTAACAAGGGGTGGGGGAAA (old nomenclature did not include the methionine codon: G450A, G450T, G450C, IVS3+2T>C, IVS3+4A>G, C344A, and IVS3+28-+46del; the 19 bp sequence of the deletion will not be used in future occurrences). We selected mutations that were identified in patients with PMD presenting with various degrees of clinical severity. We predicted the effect that each mutation might have on splice site utilization and on *PLP1* and *DM20* alternative splicing using information theory-based splice site models (Rogan, et al., 1998). Furthermore, we tested the functional relevance of the mutations on alternative splice site selection of *PLP1* and *DM20* in cultured skin fibroblasts prepared from patients' skin biopsies and by transient transfections into differentiating oligodendrocytes of minigene-splicing constructs carrying the selected mutations. *PLP1* and *DM20* transcript ratio was determined by RT-PCR analysis and compared with the ratio obtained with wild type sequence. We report here that the *PLP1* and *DM20* splice site strength contributes to the alternative splicing of *PLP1*.

MATERIALS AND METHODS

Selection of Mutations

Mutation nomenclature is based on GenBank Accession AAA59565.1 (protein) and the coding region of GenBank Accession M54927.1 (cDNA) according to recommendations of the Human Genome Variation Society (http://www.genomic.unimelb.edu.au/mdi/mutnomen/). Mutations c.453G>T, c.453G>C, c.453+2T>C, c.453+4A>G, c.347C>A, and c.453+28_+46del were previously described (Bridge and Wilkins, 1992; Pratt, et al., 1995; Nance, et al., 1996; Hobson, et al., 2000; Hobson, et al., 2002; Shy, et al., 2003). The c.453G>A mutation was identified by sequence analysis in the Molecular Diagnostics Laboratory at the Alfred I. duPont Hospital for Children of two separate PCR amplification products of a DNA sample obtained from a patient with the suspected diagnosis of PMD. Patients were either examined by one of us (Dr. Cambi or Dr. Garbern) or referred by a neurologist with expertise in PMD. For this study, we selected mutations that change conserved bases either at or around the *PLP1* and *DM20* 5' donor splice sites in exon 3 and intron 3. The type and location of the mutations are shown in Fig. 1. The study was performed under protocols approved by institutional review boards at the Alfred I. duPont Hospital for Children, Thomas Jefferson University, and Wayne State University. Informed consent was obtained when the information was not already published.

Database and Information Theory-based Analysis

The information theory-based matrices of donor and acceptor splice sites were developed and validated as described (Rogan, et al., 2003). We used Delila software to retrieve natural splice site sequences and create mutant sequences (Rogan, et al., 1998). The model is based on the sequences of exon/intron junctions of known genes on the (+) strand of the April 2003 version of the human genome draft sequence. The computer programs Scan, MakeWalker, and Lister, which are part of the Delila system, were used to calculate R_i values of normal and mutant splice

sites and to identify potentially activated new or preexisting cryptic sites. Access to this software is available with the Automated Splice Site Analysis server (Nalla and Rogan 2005).

The effects of nucleotide substitutions were predicted from R_i values as previously described (von Kodolitsch, et al., 1999). The criteria used for this analysis were previously validated and shown to be predictive of clinical and molecular phenotypes. Recent splice site models (Rogan, et al., 2003) that comprehensively model 5' donor and 3' acceptor splice sites throughout the genome indicate that mutations that reduce R_i below 1.6 bits would inactivate primary splice sites. Weakened splice sites with reduced R_i values (compared with the corresponding natural sites) often result in leaky splicing. The extent of the change in information content corresponds to the fold change in affinity, such that a 1 bit difference indicates at least a 2-fold change in binding strength. Finally, cryptic sites with R_i values exceeding those of the natural sites would be activated.

Construction of Splicing Constructs

Mutations were introduced into a previously described minigene splicing construct (Hobson, et al., 2002) by either of two methods: 1.) PCR amplification, digestion, and subcloning of the *Xba*I/*Kpn*I fragment of *PLP1* from the patient into an intermediate construct containing the whole *PLP1* insert and then transferring the mutation-containing *PLP1* insert into the backbone of the minigene splicing construct, or 2.) site-directed mutagenesis of the minigene splicing construct using a QuikChange Site-Directed Mutagenesis Kit (Stratagene, La Jolla, CA; http://www.stratagene.com/) according to the manufacturer's instructions. All constructs were

verified by automated fluorescent sequence analysis on a Prism 377 DNA Sequencer (Applied Biosystems, Foster City, CA; http://www.appliedbiosystems.com/).

Cell Cultures and Transfections

Human skin fibroblasts were established and cultured as described (Carango, et al., 1995). Mixed primary glial cultures were established from 1-day-old Sprague-Dawley rat brain as previously described (Huang, et al., 2002). Purified oligodendrocyte progenitor cells were obtained by shaking off the mixed cultures and by sequential immunopanning with antibodies to remove contaminating astrocytes and with a stage-specific antibody (A2B5) to select for oligodendrocyte progenitor cells. Oligodendrocyte progenitor cells were expanded in chemically defined medium containing 30% B104 medium and supplemented with human aa-PDGF (10 ng/ml) (R&D Systems, Minneapolis, MN; http://www.rndsystems.com/) and b-FGF (20 ng/ml) (R&D Systems). Precursors were plated in 6-well plates coated with poly-D-ornithine at $5x10^5$ cells per well and grown in 30% B104 conditioned media supplemented with 10 ng/ml aa-PDGF and 20 ng/ml b-FGF. Cells were transfected with 2 µg of plasmid DNA in 10 µl of LipofectAMINE (Invitrogen, Carlsbad, CA; http://www.invitrogen.com/), according to the manufacturer's instructions. After 5 h of exposure to the DNA, cells were differentiated in N1 medium supplemented with T3 for 72 h. After 72 h in differentiation medium, most cells had differentiated.

RNA Preparation and Reverse Transcription-Polymerase Chain Reaction (RT-PCR)

RNA extraction and RT-PCR were carried out as previously described (Hobson, et al., 2002). Briefly, total RNA was prepared from cultured cells using an RNeasy Kit with QiaShredders

(Qiagen, Valencia, CA; http://www1.qiagen.com/), treated with DNaseI (Ambion, Austin, TX; http://www.ambion.com/) according to the manufacturers' instructions and then quantitated in a 96-well format using RiboGreen (Invitrogen) and a CytoFluor multi-well plate reader (Applied Biosystems), following manufacturers' instructions.

Total RNA was denatured by heating to 65°C for 5 min in the presence of dNTPs and oligo$(dT)_{15}$ in a 12.5 µl volume. First strand cDNA synthesis was performed by reverse transcription for 30 min at 42°C in a 20 µl reaction volume containing $\leq$1 µg RNA and AMV-RT. The PCR reactions were performed with 1 to 3 µl cDNA from the RT reaction in a 50 µl reaction containing Taq Buffer, 5% DMSO, 1.5mM dNTPs, 25pmol of each primer (one primer Cy5-labeled), and 1.25U AmpliTaq polymerase (Applied Biosystems). The following temperature profile was used: 5 min melting at 94°C, amplification for 30 sec at 94°C, 30 sec at 55°C, 1 min at 65°C for 25 to 35 cycles, and a final extension of 6 min at 65°C. The primers used for PCR amplifications of RNA prepared from transfected oligodendrocytes were previously reported (Hobson, et al., 2002). Primers used for detection of endogenous products in RNA prepared from skin fibroblasts were as follows:

PLP3F6-Cy5: 5'-TGGGAAAATGGCTAGGACATCCCG (16260-16283, Acc. No. Z73964.2)

PLP5R2-Cy5: 5'- AGGGAAAGCATTCCATGGGAGAAC (18024-18001, Acc. No. Z73964)

hGAPDHF: 5'-GGTGAAGGTCGGAGTCAACG (1461-1480, Acc. No. J04038.1)

GAPDHF: 5'-GGTCGGTGTGAACGGATTTG (80-99, Acc. No. X02231.1)

GAPDHR-Cy5: 5'-GAGATGATGACCCTTTTGGC (3760-3741, Acc. No. J04038.1; 430-411, Acc. No. X02231.1)

The RT-PCR products were separated on 4% NuSieve 3:1 agarose gels (Cambrex Bio Science Rockland, Inc, Rockland, ME; http://www.cambrex.com/), and band intensities were captured

and quantitated on a Storm Phosphorimaging System (Amersham Biosciences, Piscataway, NJ; http://www4.amershambiosciences.com/aptrix/upp01077.nsf/content/homepage_country_select). The ratios of *PLP1* to *DM20* for transfection and endogenous products were calculated using data from primer pairs that distinguish *PLP1* and *DM20* by size. The *PLP1* signal plus half of the heteroduplex signal was divided by the *DM20* signal plus half of the heteroduplex signal. The heteroduplex is a hybrid between a *PLP1* and *DM20* molecule (Hobson, et al., 2002). Relative *PLP1* levels were calculated using data from a primer pair that amplifies *PLP1*-specific product only and another primer pair that amplifies a region that is common to both *PLP1* and *DM20* (*PLP1 + DM20*) as follows. To control for efficiency of transfection, we divided the *PLP1*-only signal from each transfected construct by the *PLP1 + DM20* signal. Then, to standardize the results, we divided the result for each sample by the result of the ratio obtained with the normal control transfected into differentiated oligodendrocytes.

RESULTS

Patients and Clinical Phenotypes

The phenotypes of patients carrying mutations c.453G>T, c.347C>A, c.453+2T>C, c.453+4A>G, and c.453+28_+46del were previously reported (Bridge and Wilkins, 1992; Pratt, et al., 1995; Nance, et al., 1996; Hobson, et al., 2000; Hobson, et al., 2002). Table 1 summarizes the clinical phenotypes associated with these mutations. Nucleotide changes at the conserved c.453G that is the last base of the exon and is in the 5' *PLP1* donor site are associated with a consistently severe phenotype characterized by inability to walk, hypotonia, and poor somatic growth. Since c.453G>A does not cause amino acid substitution, whereas c.453G>T and c.453G>C both cause the same amino acid substitutions p.Lys151Asn (formerly K150N or

Lys150Asn), we reason that the severe clinical effect of the c.453G mutations is unrelated to the amino acid substitution and it may result from an alteration in splicing caused by mutation in the 5' natural splice site. Nucleotide substitution in intron 3 downstream of the 5' donor splice site of *PLP1* of the almost invariant +2T position and at the conserved +4G position were still associated with a severe phenotype, since these patients never reached full motor milestones, were hypotonic and unable to walk, and had poor somatic growth. The patient carrying the c.453+2T>C mutation was reported to be able at one point to stand with assistance.

The intra-exonic nucleotide change c.347C>A is predicted to significantly strengthen the *DM20* 5' donor splice site (Table 1). In addition, the nucleotide change causes a conservative amino acid substitution of pThr117Lys in both DM20 and PLP1 protein products. This mutation is associated with a mild clinical phenotype. This subject was delayed in acquisition of motor milestones but acquired the ability to walk independently, then lost acquired motor and cognitive milestones in later years. In agreement with the clinical presentations, magnetic resonance imaging (MRI) showed severe hypomyelination very early in development and atrophy in the severely affected patients and showed dysmyelination in the patient carrying mutation c.347C>A (Nance, et al., 1996). The phenotype of the patient carrying the c.453+28 +46del is characterized by mild developmental delay in acquisition of motor milestones but ability to walk that was lost in the early teens (Hobson, et al., 2002). The MRI showed diffuse dysmyelination in subcortical white matter and optic nerves. The phenotype of the patient carrying c.347C>A is similar to that of the patient carrying the c.453+28 +46del, as both present with a mild neurological phenotype but have progressive deterioration of neurological deficits. This phenotype is highly reminiscent of that of patients with the PLP1 null syndrome (Garbern, et al., 1997; Garbern, et al., 2002).

Information Theory Analysis of Splice Site Mutations

Analysis of exon 3 sequences with information theory-based analysis identified 14 potential splice donor sites within 200bp on either side of the mutations analyzed (Table 2). Two of the donor splice sites, positions c.348G and c.453G, correspond respectively to the *DM20* and the *PLP1* splice sites. The R_i values of the natural *DM20* and *PLP1* sites are respectively 5.4 and 6.8 bits. The *PLP1* donor site is approximately average strength, on the basis of an analysis of 111,772 donor splice sites, which showed this to be 6.73 bits (Rogan, et al., 2003). The *DM20* site is 1.4 bits (or at least 2.6-fold) weaker. The remaining potential sites are not normally utilized by oligodendrocytes. However, we may expect that in the case of mutations that affect the R_i values of the *DM20* or *PLP1* sites, they could be recognized by the splicing machinery. The majority of these sites are considerably weaker than *DM20* and *PLP1*; however, one of these sites at c.411 between the *DM20* and *PLP1* sites has an R_i value of 6.7, which is stronger than the natural *DM20* site and comparable in strength with the *PLP1* site.

We have utilized the information theory analysis to calculate the R_i values at the *DM20*, *PLP1,* and other potential 5' donor sites for each of the mutations c.453G, c.347C>A, and c.453+2 and +4 and c.453+28_+46del. The percent reduction in affinity and fold decrease in binding constant for each splice site was also calculated as described in the methods. These data are presented in Table 1.

We have found that mutations at nucleotide c.453G all drastically reduce the R_i value of the *PLP1* site to 3.8, 2.8, and 3.5, respectively, and result in decreased percent binding affinity and binding constant of the *PLP1* 5' donor site. The R_i for *DM20* 5' donor site is unchanged and the predicted affinity constant and fold binding remain unmodified. Mutations at c.453+2 inactivate

the *PLP1* splice site and those at c.453+4 reduce its strength at least 4.3 bits (or 6-fold). The mutation c.347C>A strengthens the *DM20* 5' donor site by 2 bits (or 4-fold), with a predicted increase in the percent binding affinity and binding constant. The affinity of the *PLP1* 5' donor site is not predicted to be affected by c.347C>A. No change in splice site strength is predicted based on these splice site models at either the *PLP1* or the *DM20* 5' donor sites in the patient with the c453+28+46del. The R_i values of the remaining potential donor sites were unaffected by any of the mutations analyzed.

Therefore, the information theory analysis would predict that mutation at c.453+2 would eliminate *PLP1*-specific splicing and c.453G mutations and c.453+4 would severely disable it. We could not predict with certainty whether the decrease in *PLP1* splicing would lead to utilization of a cryptic site or to greater utilization of the *DM20* splice site; however, previous information analyses of analogous cryptic splicing mutations are consistent with this possibility (Rogan, et al., 1998). On the other hand, the information theory analysis predicts that the mutation c.347C>A would greatly increase the R_i of the *DM20* site from 5.4 to 7.4, while leaving unaffected the *PLP1* and other potential splice sites. This predicted increase in strength of the *DM20* 5' splice raises it above that of the natural *PLP1* site.

Molecular Phenotypes of Splicing of the Splice Site Mutations in Skin Fibroblasts

We established fibroblast cultures from skin biopsies obtained from patients with c.453G>T, c.453+2 and +4, and c.347C>A mutations and studied the effect of these mutations on RNA splicing by RT-PCR analysis. We found that *PLP1*-specific product is detected in RNA from a normal control, but it is not detected in patients with c.453G>T, c.453+2, and c.347C>A mutations and it is significantly reduced in the patient with c.453+4 mutation (Fig. 2). As an

internal control, we have carried out RT-PCR in skin fibroblasts obtained from a patient with c.453+28-+46del, and we found that the *PLP1* product is reduced. This result is in keeping with our previous findings in transfections into oligodendrocytes (Hobson, et al., 2002). Since the *PLP1* gene is expressed at low level in fibroblasts and only a small amount of *PLP1* transcript is made in these cells, we assessed the sensitivity of the RT-PCR in detecting reduction in the *PLP1*-specific product by testing a serial dilution of the normal RT product by PCR. We found that we can detect an 81-fold reduction of the normal signal, but not a 243-fold reduction. The *PLP1*-specific signal for the c.453+4 mutation is approximately equal to the 81-fold reduced signal. The signal for the *PLP1* product in fibroblasts with c.453+28-+46del was higher falling between the 27- and 81-fold reduction and was in keeping to the reduction that we reported by transfections into oligodendrocytes (Hobson, et al., 2002).

Molecular Phenotypes of the Splice Site Mutations in Oligodendrocytes

Since *PLP1* and *DM20* alternative splicing is cell-specific and highly regulated in oligodendrocytes (LeVine, et al., 1990; Stecca, et al., 2000), we have utilized a transfection paradigm into differentiating oligodendrocytes in vitro (Hobson, et al., 2002) to characterize the effect that mutations at c.453G, c.453+2 and +4, and c.453C>A have on *PLP1* and *DM20* alternative splicing. We have introduced each mutation in a chimeric mini-gene construct containing the sequence from *PLP1* exon 2 through exon 4 inserted in-frame into the bacterial *neo* gene driven by a Rous sarcoma virus (RSV) promoter (Hobson, et al., 2002) (Fig. 3A). Oligodendrocyte progenitor cells were transfected with the minigene plasmid DNAs and differentiated for 72 hours, total RNA was extracted, and transcripts were analyzed by RT-PCR using primers that amplify only plasmid-derived *PLP1/DM20* products (Fig. 3A). The *PLP1* and

DM20 splice products were amplified as products of different sizes by using primers in the *neo* sequence (neoF and neoR), and they were amplified together in the same size product by using a primer in the neo sequence and a primer in the region of exon 3 common to both products (neoF and PLPR4) (Fig. 3B). Quantitation of the *PLP1*-specific product was obtained by using a primer specific for exon3B, the *PLP1*-specific portion of exon 3, and a primer specific for neo (PLPF3 and neoR) (Hobson, et al., 2002). The endogenous *PLP1* and *DM20* transcripts were analyzed to ensure that the cells were differentiated using the same RT reaction with primers specific for *PLP1* exon 2 and 4 sequences that are not contained in the *PLP1-neo* mini-gene, and endogenous GAPDH was amplified to ensure that differences in amplified product were not the result of differences in amount of RNA (Fig. 3C).

We found that the *PLP1*-specific splice product is not detected in RNA extracted from oligodendrocytes transfected with plasmids containing the c.453G and c.453+2 mutations (Fig. 3B). On the other hand, the PLP1-specific splice product was greatly reduced in RNA of oligodendrocytes transfected with the construct containing the mutation at c.453+4 or c.347C>A (Fig. 3B and Table 1). We performed RT-PCR on RNA of oligodendrocytes transfected with a construct containing the c.453+28_+46del and obtained approximately 80% reduction of the *PLP1*-specific splice product as previously reported (Hobson, et al., 2002). These results are consistent with those obtained using RNA prepared from cultured skin fibroblasts except for c.347C>A. In the case of the c.347C>A mutation, we were able to detect *PLP1*-specific product in the transfected oligodendrocytes, but not in the skin fibroblasts. The greater sensitivity in detecting the *PLP1*-specific product is explained by the use of the oligodendrocytes in which the *PLP1*-specific splicing is highly regulated.

We were not able to determine whether the reduction of *PLP1* resulted in a compensatory increase in *DM20.* The PLP signal strength with the normal construct is low relative to *DM20* and addition of the decreased portion of this low signal due to the c.347C>A mutation to the already much higher *DM20* signal is expected to make only a subtle change in the *DM20* signal. The variability inherent in gene transfer, especially into primary cells, does not allow us to detect a subtle increase.

A PCR product smaller in size than the *PLP1*-specific product was observed in RT-PCR amplification with the exon 3B forward primer in RNA extracted from oligodendrocytes transfected with constructs carrying the c.453G>A, c.453G>C, c.453+2, and, in some instances, c.453+4 mutations. The product was sequenced and found to be generated by the use of a 5' cryptic donor site between the *DM20* and *PLP1* sites at position c.411 joining the 3' acceptor site in exon 4 (Fig. 3B). No evidence for cryptic splicing was found at any of the other potential donor sites in Table 2, but this was not surprising since they are all considerably weaker than these three sites.

DISCUSSION

In this paper, we present bioinformatics and experimental evidence that the strength of each *PLP1* and *DM20* 5' donor site plays an important role in *PLP1* alternative splicing in oligodendrocytes. We have shown that *PLP1*-specific splice site selection is reduced by mutations that either increase *DM20* splice site strength or reduce the *PLP1* splice site strength, showing that the balance between selection of the two sites is, at least in part, regulated by the splice site strength.

Our results point to some interesting aspects of the regulation of *PLP1* and *DM20* splice site selection. Mutations that were analyzed in this paper were all identified in patients with PMD and therefore reflect the natural occurrence of mutations at the *PLP1* and *DM20* splice sites. To date, of all mutations identified by our molecular diagnostics laboratory (Hobson, unpublished observations) and those reported in the literature, none has ever been found that would reduce or abolish the *DM20* splice site. In contrast, mutations in and around the *PLP1* splice site occur more frequently. We report that three different mutations at the same nucleotide (c. 453) and two point mutations and a deletion in intron 3 either severely reduce or completely abolish the *PLP1* site. The absence of naturally occurring mutations that either reduce or abolish the *DM20* splice site may indicate that these mutations are incompatible with life in the hemizygous males. The *DM20* splice site is more broadly utilized and in the CNS it is utilized early during embryonic development prior to oligodendrocyte differentiation and myelination, suggesting a more general function of *DM20* compared with *PLP1* (Campagnoni and Skoff, 2001). In contrast, *PLP1*-specific splicing occurs at high levels only in oligodendrocytes and in the postnatal period, supporting a specific function in glia and glial interactions (LeVine, et al., 1990; Stecca, et al., 2000; Sporkel, et al., 2002). Therefore, mutations that interfere with *PLP1*-specific splicing would be compatible with life and might generate a uniquely neurological phenotype. Alternatively, mutations at the *DM20* splice site may cause amino acid changes in DM20 and PLP1 protein or PLP1 protein only that are incompatible with life. This seems an unlikely alternative, however, because the c.347C>A mutation that causes a p.Thr116Lys (formerly T115K or Thr115Lys) amino acid change in both DM20 and PLP1 proteins results in a relatively mild phenotype, and most mutations that affect amino acids in the PLP1-specific region result in a mild phenotype (Cailloux, et al., 2000).

Invariably, all mutations at the highly conserved c.453G nucleotide severely reduce the *PLP1* donor site and are associated with a severe phenotype regardless of whether the mutation results in an amino acid change, suggesting that the alteration in *PLP1* splicing is the cause of disease. To elucidate the mechanism of disease severity, we have investigated whether a cryptic splice site in exon 3B is utilized leading to the synthesis of an aberrant protein product. Such a protein product may cause gain of function and result in apoptosis of the oligodendrocytes.

The information theory analysis predicts a cryptic splice site with an R_i of 6.7 located in exon 3B between *DM20* and *PLP1* sites. This site is predicted to be stronger than the *DM20* splice site (R_i of 5.4) and almost as strong as the *PLP1* splice site (R_i of 6.8). Our results suggest that the cryptic site is recognized but less efficiently than the *DM20* site despite its greater strength. A potential explanation for the efficient use of *DM20* rather than the stronger cryptic site is that donor site recognition is processive and the *DM20* site is encountered first by the splicing machinery (Robberson, et al., 1990; Niwa, et al., 1992). It is also possible that the cryptic splice site is poorly recognized by the splicing machinery because of poor accessibility due to secondary RNA structure or occupancy of the sequence by protein complexes. In this regard, the cryptic donor site has the sequence GGgt which in another gene has been shown to bind hnRNP H and thus compete for binding with the U1 snRNP of the splicing machinery (Buratti, et al., 2004). In addition, the very similar GGGGT sequence has been shown to bind hnRNP H and inhibit splicing in some contexts (Romano, et al., 2002). We have noticed some variability in the presence and amount of the transcript produced from the cryptic site, which may reflect the limitations of the in vitro transfection system. As the *PLP1* to *DM20* ratio produced by transfection does not reach the endogenous *PLP1* to *DM20* ratio, the transfection system may not produce as much cryptic product as may be seen in vivo.

The severity of the phenotype in c.453 mutations is in stark contrast with the milder phenotype observed in knockin mice carrying a mutation at c.453+1 that inactivates the *PLP1* site (Stecca, et al., 2000). It is possible that the more severe phenotype in humans may reflect species differences rather than differences in splicing regulation. Another possibility is that a cryptic site in exon 3 is utilized in humans and not in mice. The mouse exon 3B sequences contain the cryptic site; however, products derived from the cryptic site were not characterized in the mouse model (Stecca, et al., 2000 and personal communication).

We report that a mutation at the *DM20* site strengthens the *DM20* donor site and reduces *PLP1* splicing and is associated with a mild clinical phenotype. Since the *PLP1*-specific product is significantly reduced, it is unclear why the phenotype is milder than that observed with the c.453+4 mutation that seems to reduce *PLP1* splicing to a similar extent. A potential explanation is that the c.347C>A mutation causes an amino acid substitution in both PLP1 and DM20 protein products. However, PLP1 protein product, according to our data, would be significantly reduced because of inefficient splicing. The reduction in the amount of PLP1 protein would decrease the load of mutated DM20 and PLP1 proteins that traffic through and get arrested in the rough endoplasmic reticulum (RER) with consequent induction of the unfolded protein response (UPR) and apoptosis (Southwood, et al., 2002). Alternatively, it is possible that sufficient PLP1/DM20 protein is properly trafficked and inserted into the membrane resulting in survival of the oligodendrocytes and a milder phenotype.

Although the *DM20* transcript is more ubiquitously expressed, whereas *PLP1* is expressed at high levels only in oligodendrocytes, the strength of the *DM20* splice site is lower than that of *PLP1*. This raises the issue of what regulates preferential expression of the *PLP1* transcript in oligodendrocytes. Selection of *PLP1* appears to be dependent on high levels of *PLP1* gene

transcription and on an element downstream of the *PLP1* site (c.453+28+46) in oligodendrocytes. In this regard, we confirm our previous report that the c.453+28+46del mutation reduces *PLP1*-specific splicing (Hobson, et al., 2002) and demonstrate that the mutation is not predicted to change the strength of the *PLP1* and *DM20* splice sites. Previously, we suggested that selection of *PLP1* may be dependent on an intronic splicing enhancer that is deleted by the mutation. It is conceivable that low level of *PLP1* gene expression and lack of factor binding to the intronic enhancer may inhibit *PLP1* splice site selection in non-glial cells. The information theory prediction of splice donor sites suggests another possible scenario. Two potential splice donor sites are deleted by the mutation (Table 2). The deleted splice site at position c.453+34 is weak (R_i of 0) and may not have an effect, but the one at position c.453+36 is slightly stronger than the *DM20* site and is only 1.3 bits or 2.5-fold less than that of the *PLP1* site. When one or both of these sites are present, they may help to recruit the splicing machinery to the region in oligodendrocytes. In this case, silencers of *PLP1* splice site selection may be necessary in non-glial cells to prevent recognition of the *PLP1* splice site.

Overall, our data demonstrate that selection of *PLP1* and *DM20* 5' competing splice sites is in part regulated by the strength of the individual sites and suggest that additional elements regulate cryptic splice sites utilization and exclusion. The information-based theory is a very valuable tool in the analysis of splice sites and consequences of mutations at splice sites; however, further refinement will be needed to reliably predict the reciprocal effects that a mutation in one site may have on the selection of the competing splice site. Models of binding sites recognized serine and arginine (SR) rich splicing regulatory proteins are now available (Nalla and Rogan, 2005). However it is not clear yet how to quantitatively predict the combined effects of SR protein and splicesomal recognition on mRNA splicing. A combination of informatics and experimental

analyses, such as those presented in this paper, may lead to the development of algorithms that will facilitate novel quantitative approaches that more comprehensively predict the effects of splicing mutations.

ACKNOWLEDGMENTS

We acknowledge Nemours and the National Institutes of Health 1P20RR020173-01 for generously supporting GMH and KS, PHS grant ES 10855-02 for supporting PKR, Health Research Grant, State of PA, for supporting FC and ZH, and the Children's Research Center of Michigan for support to JG. We are very grateful to the PMD Foundation, the Kylan Hunter Foundation, and all the patients and families for their support and cooperation.

REFERENCES

Bridge PJ, Wilkins PJ. 1992. The role of proteolipid protein gene mutations in Pelizaeus-Merzbacher disease. Am J Hum Genet 51:A209. Abstract.

Buratti E, Baralle M, De Conti L, Baralle D, Romano M, Ayala YM, Baralle FE. 2004. hnRNP H binding at the 5' splice site correlates with the pathological effect of two intronic mutations in the NF-1 and TSHbeta genes. Nucleic Acids Res 32:4224-4236.

Cailloux F, Gauthier-Barichard F, Mimault C, Isabelle V, Courtois V, Giraud G, Dastugue B, Boespflug-Tanguy O. 2000. Genotype-phenotype correlation in inherited brain myelination defects due to proteolipid protein gene mutations. Clinical European Network on Brain Dysmyelinating Disease. Eur J Hum Genet 8:837-845.

Campagnoni AT. 1988. Molecular biology of myelin proteins from the central nervous system. J Neurochem 51:1-14.

Campagnoni AT, Skoff RP. 2001. The pathobiology of myelin mutants reveal novel biological functions of the MBP and PLP genes. Brain Pathol 11:74-91.

Carango P, Funanage VL, Quirós RE, Debruyn CS, Marks HG. 1995. Overexpression of DM20 messenger RNA in two brothers with Pelizaeus-Merzbacher disease. Ann Neurol 38:610-617.

Elrick LL, Humphrey MB, Cooper TA, Berget SM. 1998. A short sequence within two purine-rich enhancers determines 5' splice site specificity. Mol Cell Biol 18:343-352.

Garbern JY, Cambi F, Tang X-M, Sima AAF, Vallat JM, Bosch EP, Lewis R, Shy M, Sohi J, Kraft G, Chen KL, Joshi I, Leonard DGB, Johnson W, Raskind W, Dlouhy SR, Pratt V, Hodes ME, Bird T, Kamholz J. 1997. Proteolipid protein is necessary in peripheral as well as central myelin. Neuron 19:205-218.

Garbern JY, Yool DA, Moore GJ, Wilds IB, Faulk MW, Klugmann M, Nave KA, Sistermans EA, van der Knaap MS, Bird TD, Shy ME, Kamholz JA, Griffiths IR. 2002. Patients lacking the major CNS myelin protein, proteolipid protein 1, develop length-dependent axonal degeneration in the absence of demyelination and inflammation. Brain 125:551-561.

Hobson GM, Davis AP, Stowell NC, Kolodny EH, Sistermans EA, de Coo IFM, Funanage VL, Marks HG. 2000. Mutations in noncoding regions of the proteolipid protein gene in Pelizaeus-Merzbacher disease. Neurology 55:1089-1096.

Hobson GM, Huang Z, Sperle K, Stabley DL, Marks HG, Cambi F. 2002. A PLP splicing abnormality is associated with an unusual presentation of PMD. Ann Neurol 52:477-488.

Huang Z, Tang XM, Cambi F. 2002. Down-regulation of the retinoblastoma protein (rb) is associated with rat oligodendrocyte differentiation. Mol Cell Neurosci 19:250-262.

Humphrey MB, Bryan J, Cooper TA, Berget SM. 1995. A 32-nucleotide exon-splicing enhancer regulates usage of competing 5' splice sites in a differential internal exon. Mol Cell Biol 15:3979-3988.

Lees MB, Bizzozero OA. 1991. Structure and acylation of proteolipid protein. In: Martenson RE, editor. Myelin: Biology and Chemistry. Boca Raton: CRC Press. p 237-255.

LeVine SM, Wong D, Macklin WB. 1990. Developmental expression of proteolipid protein and DM20 mRNAs and proteins in the rat brain. Dev Neurosci 12:235-250.

Nalla VK, Rogan PK. 2005. Automated splicing mutation analysis by information theory. Hum Mutat 25:334-342.

Nance MA, Boyadjiev S, Pratt VM, Taylor S, Hodes ME, Dlouhy SR. 1996. Adult-onset neurodegenerative disorder due to proteolipid protein gene mutation in the mother of a man with Pelizaeus-Merzbacher disease. Neurology 47:1333-1335.

Nave KA, Lai C, Bloom FE, Milner RJ. 1987. Splice site selection in the proteolipid protein (PLP) gene transcript and primary structure of the DM-20 protein of central nervous system myelin. Proc Natl Acad Sci USA 84:5665-5669.

Niwa M, MacDonald CC, Berget SM. 1992. Are vertebrate exons scanned during splice-site selection? Nature 360:277-280.

Orkin SH, Sexton JP, Goff SC, Kazazian HH, Jr. 1983. Inactivation of an acceptor RNA splice site by a short deletion in beta-thalassemia. J Biol Chem 258:7249-7251.

Pratt VM, Naidu S, Dlouhy SR, Marks HG, Hodes ME. 1995. A novel mutation in exon 3 of the proteolipid protein gene in Pelizaeus-Merzbacher disease. Neurology 45:394-395.

Robberson BL, Cote GJ, Berget SM. 1990. Exon definition may facilitate splice site selection in RNAs with multiple exons. Mol Cell Biol 10:84-94.

Rogan PK, Faux BM, Schneider TD. 1998. Information analysis of human splice site mutations. Hum Mutat 12:153-171.

Rogan PK, Svojanovsky S, Leeder JS. 2003. Information theory-based analysis of CYP2C19, CYP2D6 and CYP3A5 splicing mutations. Pharmacogenetics 13:207-218.

Romano M, Marcucci R, Buratti E, Ayala YM, Sebastio G, Baralle FE. 2002. Regulation of 3' splice site selection in the 844ins68 polymorphism of the cystathionine Beta -synthase gene. J Biol Chem 277:43821-43829.

Shy ME, Hobson G, Jain M, Boespflug-Tanguy O, Garbern J, Sperle K, Li W, Gow A, Rodriguez D, Bertini E, Mancias P, Krajewski K, Lewis R, Kamholz J. 2003. Schwann

cell expression of PLP1 but not DM20 is necessary to prevent neuropathy. Ann Neurol 53:354-65.

Smith CW, Valcarcel J. 2000. Alternative pre-mRNA splicing: the logic of combinatorial control. Trends Biochem Sci 25:381-388.

Southwood CM, Garbern J, Jiang W, Gow A. 2002. The unfolded protein response modulates disease severity in Pelizaeus-Merzbacher disease. Neuron 36:585-596.

Sporkel O, Uschkureit T, Bussow H, Stoffel W. 2002. Oligodendrocytes expressing exclusively the DM20 isoform of the proteolipid protein gene: myelination and development. Glia 37:19-30.

Stecca B, Southwood CM, Gragerov A, Kelley KA, Friedrich VL, Jr., Gow A. 2000. The evolution of lipophilin genes from invertebrates to tetrapods: DM-20 cannot replace proteolipid protein in CNS myelin. J Neurosci 20:4002-4010.

Thompson TE, Rogan PK, Risinger JI, Taylor JA. 2002. Splice variants but not mutations of DNA polymerase beta are common in bladder cancer. Cancer Res 62:3251-3256.

Timsit S, Sinoway MP, Levy L, Allinquant B, Stempak J, Staugaitis SM, Colman DR. 1992. The DM20 protein of myelin: intracellular and surface expression patterns in transfectants. J Neurochem 58:1936-1942.

Treisman R, Orkin SH, Maniatis T. 1983. Specific transcription and RNA splicing defects in five cloned beta-thalassaemia genes. Nature 302:591-596.

von Kodolitsch Y, Pyeritz RE, Rogan PK. 1999. Splice-site mutations in atherosclerosis candidate genes: relating individual information to phenotype. Circulation 100:693-699.

Table 1. Patients with mutations that affect *PLP1/DM20* alternative splicing

Mutation		Clinical Phenotype		Molecular Phenotype	Information Analysis R_i natural → mutant (fold change; % binding)		Cryptic Site (c.411)
DNA	Amino Acid	Clinical	MRI	% PLP1 v DM20	PLP1	DM20	Utilized?
c.347C>A	p.Thr116Lys	mild	dysmyelination	2%	6.8 → 6.8	5.4 → 7.4 (4.1; 407%)	no
c.453G>A		severe	severe myelin deficit	0%	6.8 → 3.8 (-8.3 ; 12%)	5.4 → 5.4	yes
c.453G>T	p.Lys151Asn	severe	severe myelin deficit	0%	6.8 → 3.5 (-10; 10%)	5.4 → 5.4	yes
c.453G>C	p.Lys151Asn	severe	severe myelin deficit	0%	6.8 → 2.8 (-16.5; 6%)	5.4 → 5.4	yes
c.453+2 T>C		severe	atrophy and myelin deficit	0%	6.8 → -0.06	5.4 → 5.4	yes
c.453+4 A>G		severe	severe myelin deficits	4%	6.8 → 4.3 (-5.9; 16.8%)	5.4 → 5.4	no
c.453+28_+46del		mild	mild dysmyelination	20%	6.8 → 6.8	5.4 → 5.4	no

ND, not done. The data presented under % of *PLP1* versus *DM20* are expressed as the percent of the *PLP1* product obtained with each mutated construct compared with the amount of the *PLP1* product obtained with the wild type sequences. In parentheses next to the R_i values, we have shown the percent reduction and increase of binding of the mutated sites versus the wild type. Mutation nomenclature is based on GenBank Accession AAA59565.1 (protein) and the coding region of GenBank Accession M54927.1 (cDNA).

Table 2. Predicted potential splice donor sites within 200bp of the natural sites

Genomic Coordinate	cDNA Coordinate		Position relative to natural PLP1 site	R_i
g.101074376	c.206		-247	4.3
g.101074458	c.288		-165	0.3
g.101074498	c.328		-125	1.3
g.101074518	c.348	DM20	-105	5.4
g.101074536	c.366		-87	3.1
g.101074581	c.411	cryptic	-42	6.7
g.101074623	c.453	PLP1	0	6.8
g.101074657	c.453+34		34	0
g.101074659	c.453+36		36	5.5
g.101074732	c.453+109		109	1.6
g.101074736	c.453+113		113	4.2
g.101074769	c.453+146		146	6.6
g.101074781	c.453+158		158	0.2
g.101074784	c.453+161		161	0.6

Genomic coordinates refer to April 2003 version of the human genome draft sequence.
cDNA coordinates refer to GenBank Accession M54927.1.

FIGURE LEGENDS

Figure 1. A. Diagram of the *PLP1* gene with the *PLP1/DM20* alternative splice indicated. B. Diagram of the *DM20* splice (c.348), the *PLP1*-specific splice (c.453), and a cryptic splice (c.411) site. Mutations and their positions are indicated above the sequence. The *DM20* splice site is at the end of exon 3A, indicated in red; the *PLP1*-specific splice site is at the end of exon 3B, indicated in green. Exon 4 is indicated in blue. Amino acid sequence is indicated below the DNA sequence. Predicted splice site strengths are indicated. Sequences are from GenBank Accession AAA59565.1 (protein) and the coding region of GenBank Accession M54927.1 (cDNA).

Figure 2. Reverse transcription polymerase chain reaction (RT-PCR) analysis of total RNA from patient and normal cultured skin fibroblasts. Analysis of a serial 3-fold dilution of the normal RNA is also shown. The RNA (1 μg or dilution) was reverse transcribed, and PCR was performed using 5 μl of the product for 35 cycles with primers PLP3F6 and PLP5R2 that detect the *PLP1*-specific transcript or 1 μl. of the product for 25 cycles with primers that detect GAPDH.

Figure 3. Reverse transcription polymerase chain reaction analysis of total RNA from differentiated rat primary oligodendrocytes (OL) transfected with mutant and normal constructs. A. Splicing construct showing the *PLP1* and *DM20* alternative splice. Part of *PLP1* exon 2 through part of exon 4 was inserted into the *neo* gene driven by the Rous sarcoma virus (RSV) promoter. Arrowheads indicate the locations of primers used for polymerase chain reaction

amplification. B. The RNA (43 to 85 ng, amount remained constant within each experiment) was reverse transcribed, and PCR was performed using 2 or 3 μl of the product for 30 cycles with primers neoF and neoR to detect both *PLP1* and *DM20* from the transfected constructs and with primers PLPF3 and neoR to detect *PLP1* only from the transfected constructs. C. The RNA was reverse transcribed, and PCR was performed with primers PLPF4 and PLPR2, which are outside the region of *PLP1* contained within the splicing construct, to detect endogenous rat *Plp1* and *DM20*, or with primers GAPDHF and GAPDHR for 25 cycles to detect endogenous rat GAPDH expression. All PCR products were obtained by amplification of cDNA obtained from the same RT reaction. The slower migrating band labeled as heteroduplex is a hybrid between a *PLP1* and a *DM20* molecule. The relative *PLP1* levels were calculated as described (Materials and Methods). This is one of two independent transfections utilizing two separate primary oligodendrocyte cell preparations. Transfections were performed in duplicate dishes and pooled for each data point. A reduced level of *PLP1* expression is seen from the c.453+4A>G, c.347C>A, and c.453+28-+46 constructs and no *PLP1* is seen from the c.453+2T>C and the c.453G constructs. Mutation nomenclature is based on the coding region of GenBank Accession M54927.1 (cDNA).

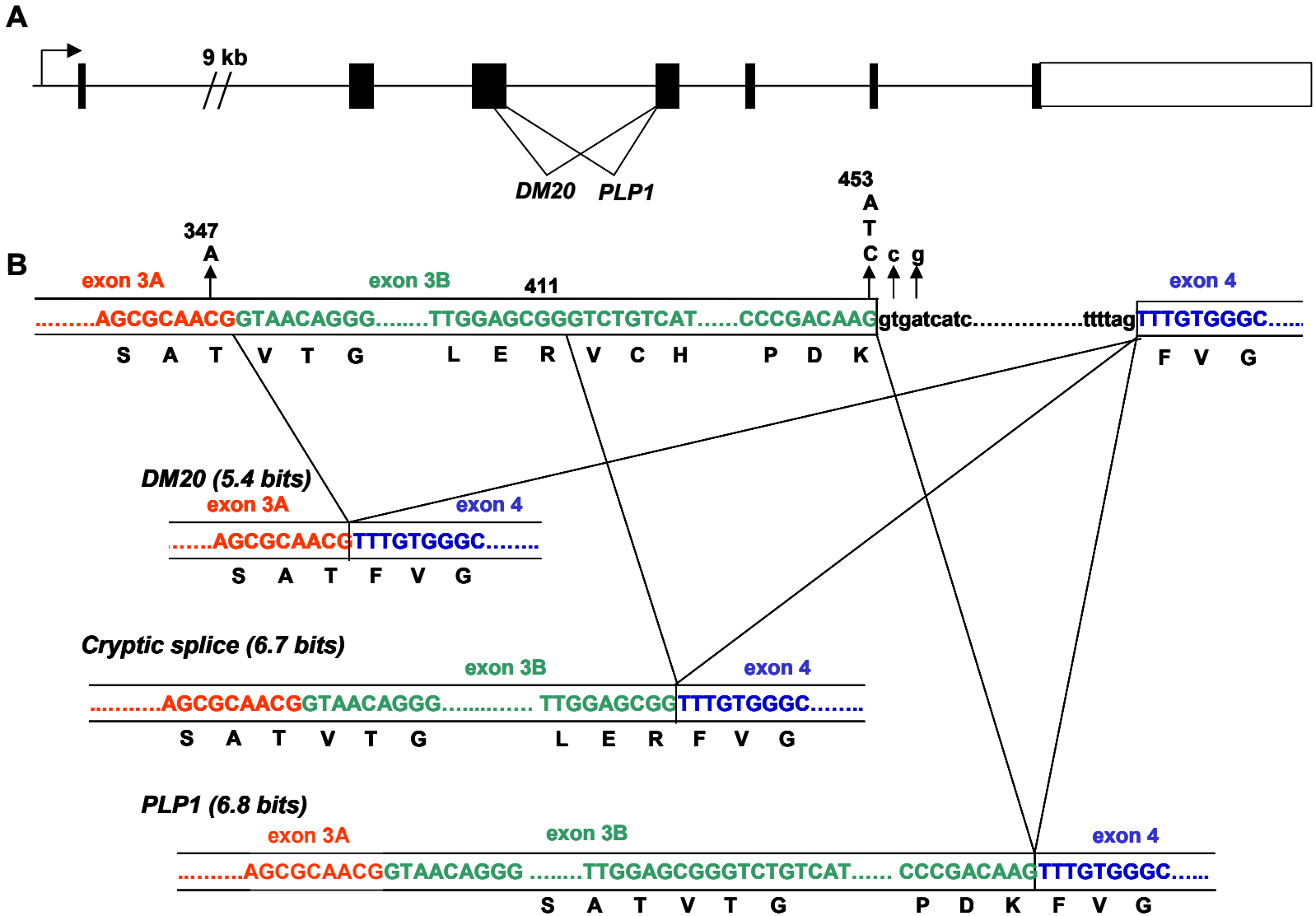
A
9 kb
DM20
PLP1
B
347
A
453
A
T
C c g
exon 3A
exon 3B
411
exon 4
.....AGCGCAACGGTAACAGGG.....TTGGAGCGGGTCTGTCAT.....CCCGACAAGgtgatcatc.....ttttagTTTGTGGGC.....
S A T V T G L E R V C H P D K F V G
DM20 (5.4 bits)
exon 3A
exon 4
.....AGCGCAACGTTTGTGGGC.....
S A T F V G
Cryptic splice (6.7 bits)
exon 3B
exon 4
.....AGCGCAACGGTAACAGGG..... TTGGAGCGGTTTGTGGGC.....
S A T V T G L E R F V G
PLP1 (6.8 bits)
exon 3A
exon 3B
exon 4
.....AGCGCAACGGTAACAGGG .....TTGGAGCGGGTCTGTCAT..... CCCGACAAGTTTGTGGGC.....
S A T V T G P D K F V G

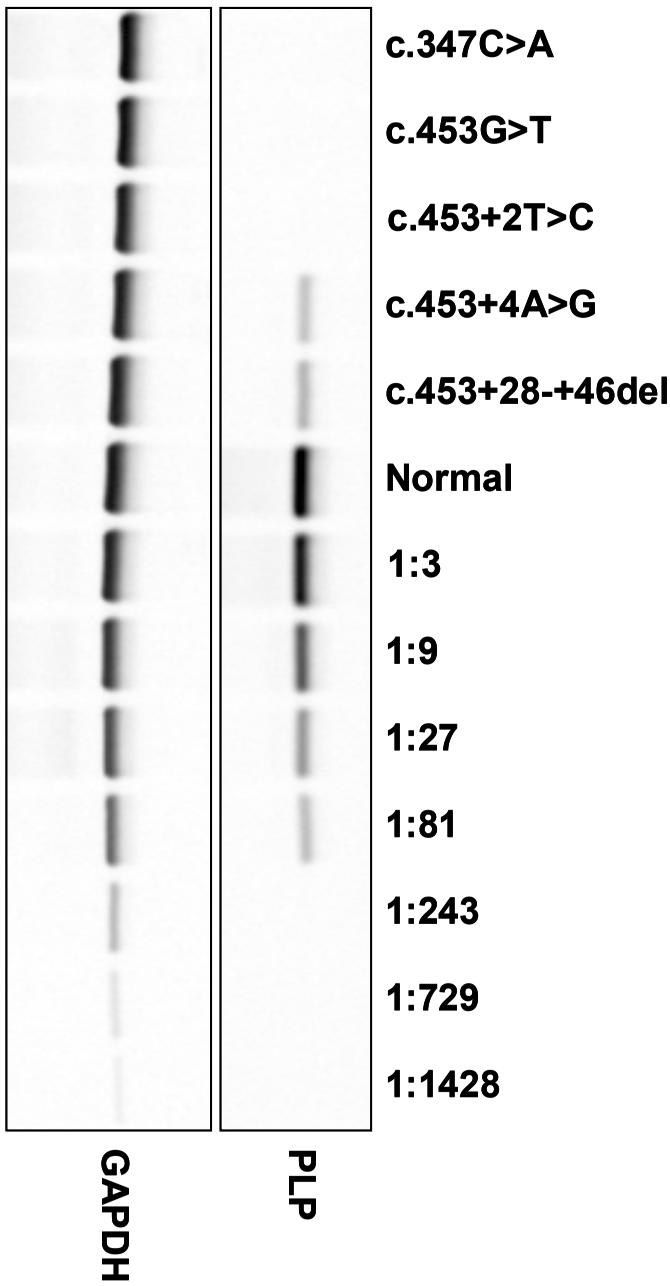
c.347C>A
c.453G>T
c.453+2T>C
c.453+4A>G
c.453+28-+46del
Normal
1:3
1:9
1:27
1:81
1:243
1:729
1:1428
GAPDH
PLP

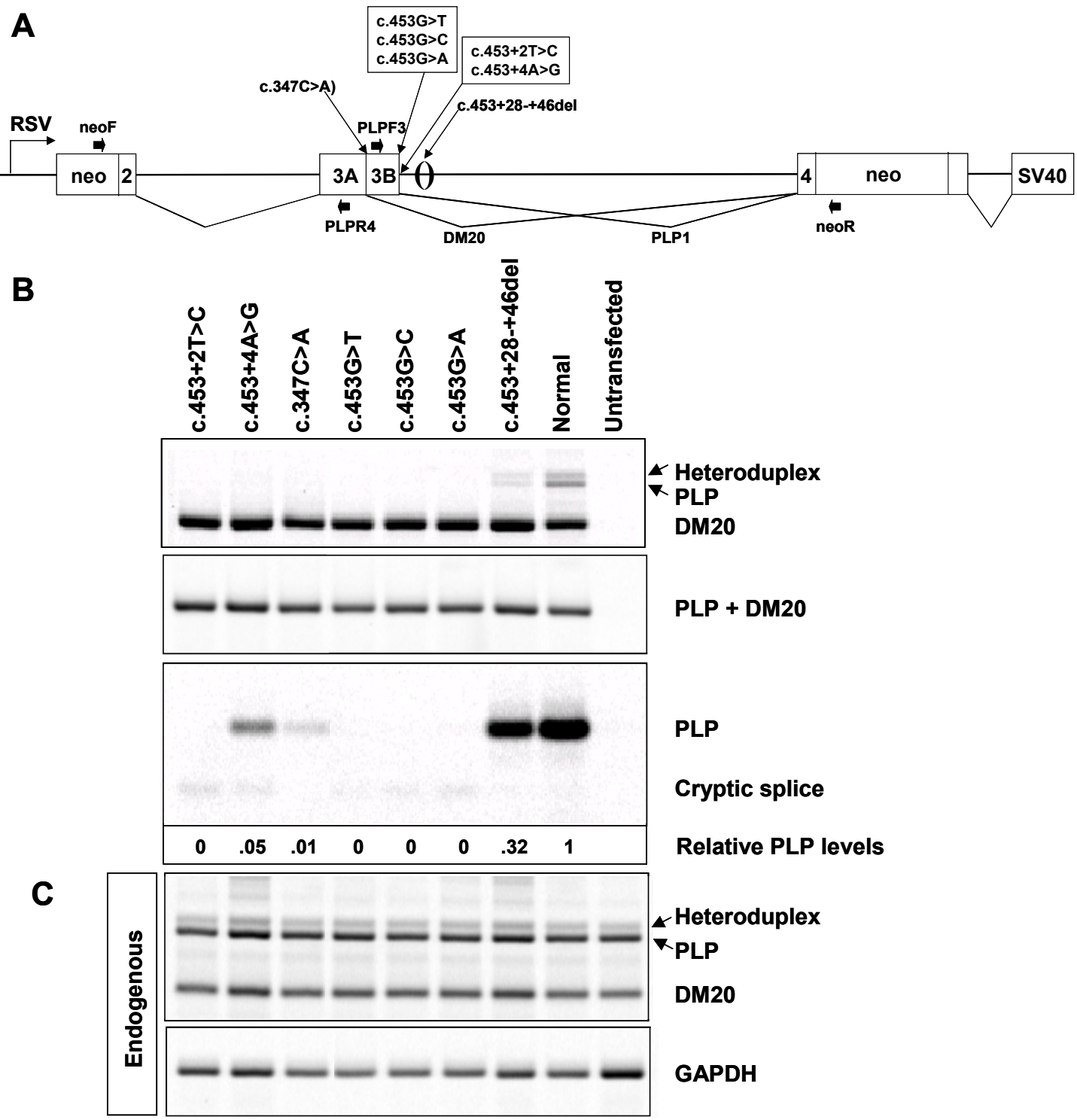
A
c.453G>T
c.453G>C
c.453G>A
c.453+2T>C
c.453+4A>G
c.347C>A)
c.453+28-+46del
RSV
neoF
PLPF3
neo
2
3A
3B
θ
4
neo
SV40
PLPR4
DM20
PLP1
neoR
B
c.453+2T>C
c.453+4A>G
c.347C>A
c.453G>T
c.453G>C
c.453G>A
c.453+28-+46del
Normal
Untransfected
Heteroduplex
PLP
DM20
PLP + DM20
PLP
Cryptic splice
0
.05
.01
0
0
0
.32
1
Relative PLP levels
C
Endogenous
Heteroduplex
PLP
DM20
GAPDH